

Dilaton Effective Field Theory across the Conformal Edge

Thomas Appelquist,^{1,*} James Ingoldby^{2,†} and Maurizio Piai^{3,4,‡}

¹*Department of Physics, Sloane Laboratory, Yale University, New Haven, Connecticut 06520, USA*

²*Institute for Particle Physics Phenomenology, Durham University, Durham DH1 3LE, UK*

³*Department of Physics, Faculty of Science and Engineering,*

Swansea University, Singleton Park, SA2 8PP, Swansea, United Kingdom

⁴*Centre for Quantum Fields and Gravity, Faculty of Science and Engineering,*

Swansea University, Singleton Park, SA2 8PP, Swansea, United Kingdom

Dilaton effective field theory (dEFT) can be employed to analyze lattice data in gauge theories that lie in close proximity of the lower edge of the conformal window. Under special conditions, we show that it can be used as a diagnostic tool to distinguish near-conformal, yet confining, theories from infrared conformal ones. We demonstrate this efficacy by analyzing two sets of lattice measurements taken from the literature. For the $SU(3)$ theory coupled to $N_f = 8$ Dirac fermions transforming in the fundamental representation, our analysis favors confinement. For the $SU(2)$ theory with $N_f = 1$ adjoint fermion, our fits favor infrared conformal behavior. We discuss future lattice measurements, and analysis refinements, that can further test this framework.

I. INTRODUCTION

In four dimensions, asymptotically free gauge theories are realized in different zero-temperature phases, depending on the type and number N_f of light matter fields included. In the absence of matter fields, Yang-Mills theories confine, and the presence of few fermions does not alter qualitatively this feature, except for introducing continuous global symmetries and their spontaneous breaking. Conversely, for a large enough number of fermions, long distance physics is governed by the appearance of an infrared fixed point, with its associated conformal invariance. This can be shown perturbatively, when N_f is close to its upper bound insuring asymptotic freedom [1]. The conformal behavior is expected to persist over a finite range of $N_f > N_{fc}$, with the lower bound defining the edge of the conformal window. The determination of N_{fc} , and the characterization of the theory near it, is an interesting strong-coupling problem.

Lattice field theory is the natural instrument to study the problem, and in recent years it has led to significant advances—see the review in Ref. [2] and references therein, as well as the more recent Refs. [3–7]. These studies explore a finite range of fermion masses that suppress infrared sensitivity to the lattice volume, and yield a discrete spectrum of bound states, as expected in confining theories. Some of these studies have reported evidence for the existence of a relatively light, flavor-singlet particle, together with a set of similarly light pseudoscalar particles, separated in mass from heavier bound states [7–28].

In a gauge theory outside of the conformal window, the pseudoscalars are naturally interpreted as pseudo-Nambu-Goldstone Bosons (pNGBs), associated with the

spontaneous breaking of an approximate internal global symmetry acting on the matter fields. With the light flavor-singlet interpreted as a dilaton associated with the spontaneous breaking of approximate dilatation symmetry, the behavior of a gauge theory taken to be just below the edge of the window has been successfully described employing dilaton effective field theory (dEFT) [29–41]. See also the review in Ref. [42] and references therein, including the precursors in Refs. [43, 44], the early study in the context of electroweak symmetry breaking [45], as well as recent phenomenological applications in Refs. [46–52], and theoretical developments in Refs. [53–58].

In this paper, we expand on this idea, noting that the same dEFT can also be used just inside the conformal window, in the presence of a finite fermion mass. The dilaton and pNGBs continue to exist there as relatively light states. Therefore, dEFT can be employed to explore near-edge gauge theories without an inside-versus-outside bias, and hence used as a diagnostic tool to discriminate between confining and conformal behavior. We test this framework by applying it to two gauge theories in proximity to the lower edge of the conformal window. We start with the well studied $SU(3)$ gauge theory with $N_f = 8$ Dirac fermions in the fundamental representation [17, 18], finding, as assumed in Refs. [29–41], that it is outside the conformal window. We then analyze the $SU(2)$ gauge theory coupled to $N_f = 1$ Dirac fermion transforming in the adjoint representation [7, 28], finding evidence that it is inside.

In Section II, we discuss the general framework. We then implement it to fit the lattice data for the above two gauge theories in Section III. In Section IV, we summarize our results and discuss future directions. We relegate to the Appendix some technical details about our fitting procedure, and tables reproducing the data we take from Refs. [17, 59] and [28, 60, 61].

* thomas.appelquist@yale.edu

† james.a.ingoldby@durham.ac.uk

‡ m.piai@swansea.ac.uk

II. DILATON EFFECTIVE FIELD THEORY

In the dEFT Lagrangian density, the canonically normalized dilaton field χ has a potential $V(\chi)$ and couplings to the pNGBs:

$$\mathcal{L} = \frac{1}{2}\partial_\mu\chi\partial^\mu\chi - V(\chi) + \frac{P}{4}\chi^2\text{Tr}[\partial_\mu\Sigma(\partial^\mu\Sigma)^\dagger] + \frac{R}{4}\chi^y\text{Tr}[\Sigma X^\dagger + X\Sigma^\dagger]. \quad (1)$$

The matrix field Σ describes the pNGBs. The factor χ^2 multiplying their kinetic term acts as a conformal compensator, and P is a positive dimensionless parameter to be fit to lattice data. The final term describes explicit breaking of the internal global symmetry arising from the finite mass m assigned to the fermions in the underlying gauge theory. The χ dependence of the terms in Eq. (1) follows from a spurion analysis, explained in Refs. [39, 42]. Heavier states and subleading interactions are neglected.

The form of Σ and the parameter matrix X are dictated by the internal symmetry and the appropriate breaking pattern. In the case of gauge theories with matter in complex representations (as with the $SU(3)$, $N_f = 8$ theory), Σ transforms on the left and right according to the $SU(N_f)_L \times SU(N_f)_R$ symmetry, and satisfies the nonlinear constraint $\Sigma\Sigma^\dagger = \mathbb{1}_{N_f \times N_f}$, while $X = \mathbb{1}_{N_f \times N_f}$.

For theories with matter in real representations, the global symmetry is enhanced to $SU(2N_f)$, and the pNGBs span the $SU(2N_f)/SO(2N_f)$ coset. Hence, $\Sigma \equiv S X = X S^T$ transforms as the symmetric representation of $SU(2N_f)$, with S satisfying $SS^\dagger = \mathbb{1}_{2N_f \times 2N_f}$, and with X symmetric and traceless. For the $SU(2)$ theory with adjoint matter ($N_f = 1$), we choose $X = \tau^1$, the first Pauli matrix.¹

The factor χ^y in the final term of \mathcal{L} is also a conformal compensator, with the scaling dimension y determined by fits to lattice data. The non-negative constant R , of dimension $4-y$, is induced by the presence of the underlying fermion mass m , defined at the lattice cutoff. It vanishes in the limit $m \rightarrow 0$, and we take its m -dependence to be linear:

$$R = B_f m, \quad (2)$$

where B_f is a positive constant.

For the dilaton potential $V(\chi)$, we adopt the form

$$V(\chi) = A\chi^4 + B\chi^\Delta, \quad (3)$$

where $\Delta (> 0)$, A , and B are real parameters, and where the second term describes the expected deformation of

conformality present even in the limit $m = 0$. The full scalar potential is given by

$$W(\chi) = V(\chi) - \frac{1}{2}xN_f R\chi^y, \quad (4)$$

with $x = 1$ for complex representations, and $x = 2$ for real and pseudo-real ones. For the case $y < 4, \Delta$, and with $R > 0$, the second term dominates for small χ , driving the system away from the origin and toward a stable, symmetry breaking minimum of $W(\chi)$.

We note in passing that our previous studies [39, 42] of the $SU(3)$ gauge theory with $N_f = 8$ fermions in the fundamental representation were conducted with a constraint on the parameters of the potential $V(\chi)$ such that it has a symmetry breaking minimum, insuring that the spontaneous breaking of approximate conformal symmetry persists in the limit $R = 0$. Here we proceed more generally, allowing lattice fits to determine whether or not $V(\chi)$ has a symmetry-breaking minimum, that is whether the theory is just outside or just inside the conformal window.

III. FITS TO LATTICE DATA

The parameters of the dEFT in Eq. (1) derive from the underlying gauge theory that UV completes it. They are directly related to the decay constants (F_d, F_π) and masses (M_d, M_π) of the dilaton and pNGBs. Lattice studies of the underlying gauge theory typically present values for these quantities as functions of a common mass m of the fermions, defined at the UV cutoff.

The quantity F_d is the vacuum expectation value (VEV) of χ , determined in terms of the dEFT parameters by extremizing $W(\chi)$:

$$4AF_d^{4-y} + \Delta BF_d^{\Delta-y} - \frac{1}{2}xN_f Ry = 0. \quad (5)$$

The dilaton mass is given by

$$M_d^2 = 12AF_d^2 + \Delta(\Delta-1)BF_d^{\Delta-2} - \frac{1}{2}xN_f Ry(y-1)F_d^{y-2}. \quad (6)$$

With $\Sigma \equiv \exp[2i\Pi/F_\pi]$, canonical normalization of the pNGB kinetic term gives

$$F_\pi^2 = PF_d^2, \quad (7)$$

and

$$M_\pi^2 = RF_d^y/F_\pi^2. \quad (8)$$

Lattice measurements exist for only the quantities F_π^2 , M_π^2 , and M_d^2 , so we reorganize the above equations to obtain three useful fit equations. The first, independent of $V_\Delta(\chi)$, is

$$M_\pi^2 F_\pi^{2-y} - Cm = 0. \quad (9)$$

¹ For pseudo-real representations, X and Σ are antisymmetric matrices, and the pNGBs describe the $SU(2N_f)/Sp(2N_f)$ coset.

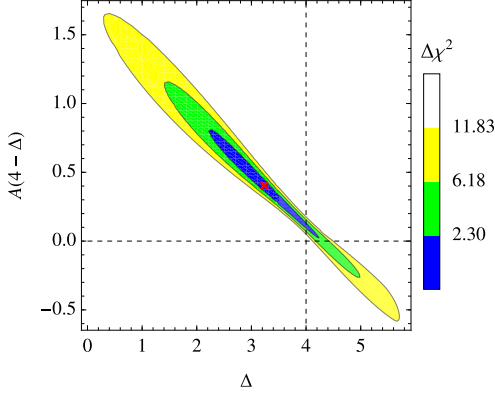


FIG. 1. Contours of $\Delta\chi^2$ indicating confidence intervals (equivalent to 1σ , 2σ , and 3σ , respectively), for A and Δ in the $SU(3)$ gauge theory with $N_f = 8$ Dirac fermions in the fundamental representation. The central value denoted by the red dot is reported in Table I. For each point of the plot, we minimize the χ^2 in respect to the other four fit parameters. The region $A > 0$ and $\Delta < 4$ is favored.

where $C \equiv B_f/P^{y/2}$ is treated as a fit parameter. Two additional equations can be obtained in which the exponential dependence on the fit parameter y is removed. They take the form

$$\frac{M_\pi^2}{F_\pi^2} - \frac{2}{yxN_fP^2} \left[4A + \Delta B \left(\frac{F_\pi^2}{P} \right)^{\frac{\Delta-4}{2}} \right] = 0, \quad (10)$$

and

$$\frac{M_d^2}{F_\pi^2} - \frac{4(4-y)A}{P} - \frac{\Delta(\Delta-y)B}{P} \left(\frac{F_\pi^2}{P} \right)^{\frac{\Delta-4}{2}} = 0. \quad (11)$$

As we employ Eqs. (9)-(11) to fit the lattice data, we will find it helpful to depict the form of $V'(\chi)$ in a way that incorporates the uncertainty in the fit parameters. Noting that $V'(F_d) = [\frac{1}{2}xyN_fP^{1/2}] M_\pi^2 F_\pi$, and employing Eq. (10), we can display the form of $V'(F_d)$, simply by plotting $M_\pi^2 F_\pi$ versus $F_\pi (= P^{-1/2} F_d)$. This plot can be extended to show the form of $V'(\chi)$ even at values of χ below a potentially non-vanishing VEV, where it is negative, by continuation of F_π to small values.

A. $SU(3)$ Gauge Theory with $N_f = 8$ Fermions in the Fundamental Representation

The lattice data obtained from Refs. [17, 59] is summarized in Table III of Appendix A. The masses and decay constants of the 63 pNGBs and the masses of the dilaton are listed there for 5 values of the underlying fermion mass m . As noted in the Appendix, correlations are neglected. The choice of lattice coupling β and the range of fermion mass m employed in the lattice study lead to

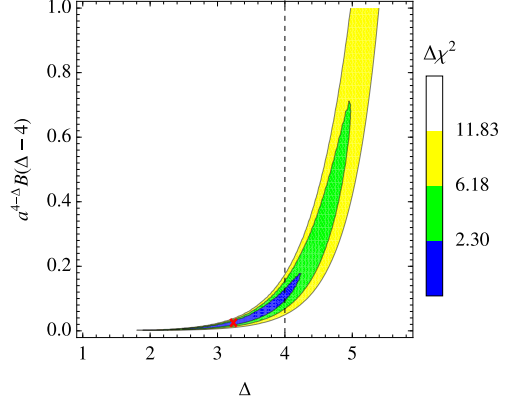


FIG. 2. Contours of $\Delta\chi^2$ indicating confidence intervals (equivalent to 1σ , 2σ , and 3σ , respectively), for B and Δ , in the $SU(3)$ gauge theory with $N_f = 8$ Dirac fermions in the fundamental representation. The central value denoted by the red dot is reported in Table I. For each point of the plot, we minimize the χ^2 in respect to the other four fit parameters. The region with $B < 0$ and $\Delta < 4$ is favored, consistent with being outside the conformal window.

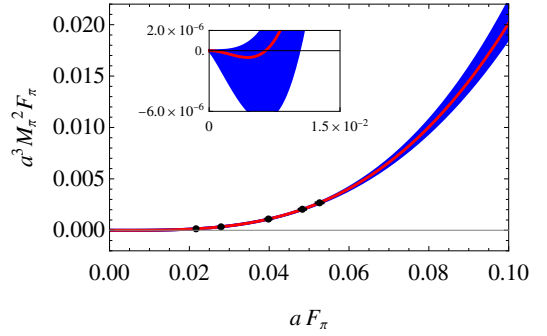


FIG. 3. Plot of $a^3 M_\pi^2 F_\pi$ versus aF_π , in the $SU(3)$ theory with $N_f = 8$ fermions in the fundamental representation [17, 59]. The red curve is based on the central values of Table I, with the five data points denoted by the black discs. The blue shaded region represents the uncertainty in the fitting curve, equivalent to the 1σ confidence level. The red curve reaches the horizontal axis at a nonzero value of aF_π , corresponding to the limit $m \rightarrow 0$ in a confining gauge theory. For larger values of $F_\pi \propto F_d$, we have $M_\pi^2 F_\pi \propto V'(F_d)$. The curve is extrapolated downward, where it becomes negative, by continuing Eq. (10) to unphysical values of F_π , demonstrating that the region near the origin is unstable, as shown in the inset.

masses M_π and M_d well below the inverse lattice spacing, and also below the masses of heavier states, which are not included in the dEFT analysis.

Results for A , B , and Δ are shown in Figs. 1 and 2 in the form of $\Delta\chi^2$ contours. The favored upper left quadrants together correspond to values $\Delta < 4$, $A > 0$, and $B < 0$. The central values of all 6 fit parameters are shown in Table I. Those for y and P are consistent

TABLE I. Central values in the dEFT fit for the $SU(3)$ gauge theory with $N_f = 8$ Dirac fermions in the fundamental representation. Lattice data for M_π , M_d , and F_π is incorporated into this fit, for 5 different values of the underlying fermion mass m , corresponding to 15 data points. The lattice measurements are taken from Refs. [17, 59], and reproduced in Table III. Dimensional quantities are presented in units of the lattice spacing, a .

Parameter	Central Value
y	2.081
$a^{3-y}C$	7.16
Δ	3.237
P	0.1050
A	0.527
$a^{4-\Delta}B$	- 0.0328
χ^2/dof	2.70 / 9

with earlier studies. The central values of Δ (< 4), A (positive), and B (negative) imply that the theory lies just outside the conformal window, with $V(\chi)$ having a symmetry breaking minimum, as assumed in our earlier studies [42].

A graphical depiction of this conclusion is shown in Fig. 3. We plot $M_\pi^2 F_\pi$ as a function of $F_\pi \propto F_d$. The red curve is based on the central values of Table I. It shows $M_\pi^2 F_\pi$ vanishing at a finite value of F_π (corresponding to $m \rightarrow 0$), and increasing continuously with increasing F_π . In this range, $M_\pi^2 F_\pi \propto V'(F_d)$. We extend the fit equations (9)-(10) into this regime. The blue shaded region represents uncertainty in the fitting curve equivalent to the 1σ level. The five data points, depicted by the black discs, lie well above the value of F_π where $V'(F_d)$ vanishes, and well within a region where the uncertainty in the fit is small.

B. $SU(2)$ Gauge Theory with $N_f = 1$ Fermion in the Adjoint Representation

We again employ Eqs. (9)-(11) to fit the lattice data [7, 28, 60, 61]. In this case, with the spontaneous breaking pattern $SU(2) \rightarrow SO(2)$, there are 2 pNGBs. We list the measurements performed with Wilson fermions and coupling $\beta = 2.1$, for the largest available volumes, in Table IV of Appendix A. We identify the fermion mass m_{PCAC} , defined following Ref. [62], with the mass parameter m in our fits. We include in our analysis only the three ensembles with the lightest mass, $aM_{\pi,d} < 0.7$. We tested the stability of the fits by including one or more

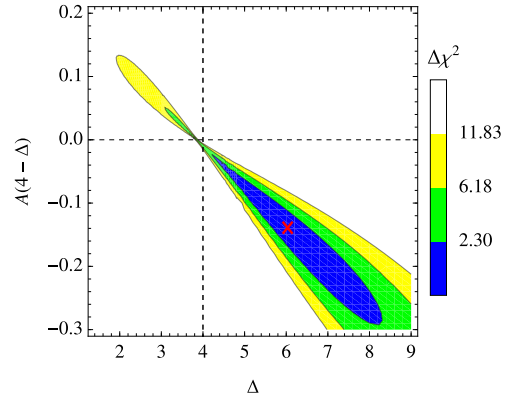


FIG. 4. Contours of $\Delta\chi^2$ indicating confidence intervals (equivalent to 1σ , 2σ , and 3σ , respectively), for A and Δ in the $SU(2)$ gauge theory with $N_f = 1$ Dirac fermion in the adjoint representation. The fit includes only data taken at the three lightest fermion mass points. The central value is reported in Table II. For each point of the plot, we minimize the χ^2 in respect to the other four fit parameters. The region with $\Delta > 4$ and $A > 0$ is favored, consistently with infrared conformal behavior.

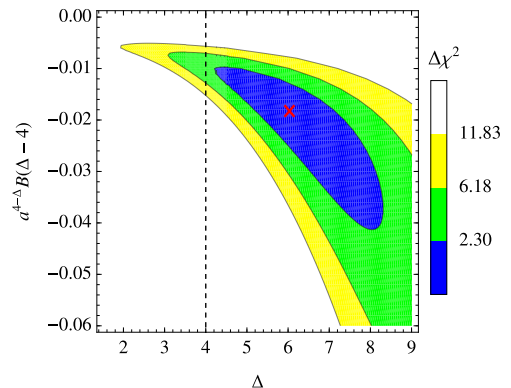


FIG. 5. Contours of $\Delta\chi^2$ indicating confidence intervals (equivalent to 1σ , 2σ , and 3σ , respectively), for B and Δ in the $SU(2)$ gauge theory with $N_f = 1$ Dirac fermion in the adjoint representation. The fit includes only data taken at the three lightest fermion mass points. The central value is reported in Table II. For each point of the plot, we minimize the χ^2 in respect to the other four fit parameters. The region with $\Delta > 4$ and $B < 0$ is favored, consistently with infrared conformal behavior.

heavier ensembles.²

² As discussed in Ref. [7], ensembles with $\beta > 2.1$ yield a systematic decrease in the anomalous dimension of the fermion condensate, indicating to us that in those ensembles the Wilson fermion mass does not reach low enough values to assess the existence of an IR fixed point.

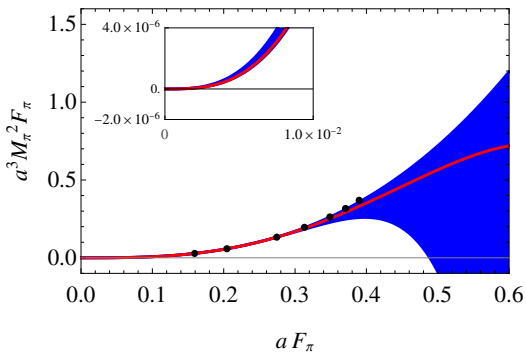


FIG. 6. Plot of $a^3 M_\pi^2 F_\pi$ versus $a F_\pi \propto a F_d$, in the $SU(2)$ theory with $N_f = 1$ fermion in the adjoint representation [28, 60, 61], restricting attention to ensembles with $\beta = 2.1$. The red curve is based on the central values of Table II, using only the three lightest ensembles. The data points are depicted by the black discs. The red curve reaches the horizontal line at $F_\pi = 0$, as shown in the inset, corresponding to the limit $m \rightarrow 0$ in an infrared conformal theory. Throughout the range, $a^3 M_\pi^2 F_\pi \propto V'(F_d)$. The blue shaded region represents the uncertainty in the fitting curve, equivalent to the 1σ confidence level.

TABLE II. Central values for the dEFT fit for the $SU(2)$ gauge theory with $N_f = 1$ Dirac fermion in the adjoint representation. The lattice data is taken from Refs. [28, 60, 61], and reproduced in Table IV, and has been restricted to the three ensembles with smallest fermion mass and $\beta = 2.1$. Lattice data for M_π , M_d , F_π , and m_{PCAC} has been incorporated into this fit, corresponding to 9 data points. Dimensional quantities are presented in units of the lattice spacing, a .

Parameter	Central Value
y	2.19
$a^{3-y} C$	7.69
Δ	6.03
P	0.131
A	0.0683
$a^{4-\Delta} B$	-0.0090
χ^2/dof	0.616/3

Results for A , B , and Δ are shown in Figs. 4 and 5 in the form of $\Delta\chi^2$ contours, with central values listed in Table II. Among the central values, those for y and P are similar to those of Table I. In particular, $y \approx 2$, as expected near the edge of the conformal window [63]. We again have $A > 0$ and $B < 0$, but now $\Delta > 4$. Thus $V(\chi)$ turns down at large χ , but the turn-down sets in well beyond the range of applicability of the dEFT.

We depict this in Fig. 6, by plotting $M_\pi^2 F_\pi \propto V'(F_d)$ as a function of $F_\pi \propto F_d$. The red curve, based on the central values of Table II, shows $V'(F_d)$ vanishing at $F_\pi = 0$ (corresponding to the limit $m \rightarrow 0$ in an infrared conformal gauge theory), and increasing with F_π through values well beyond the location of the data points, de-

icted by the black discs. The data points lie low enough so that the 1σ -fit uncertainty, represented by the shaded region, is relatively small.

We conclude that available lattice measurements indicate that this theory is inside the conformal window. It is governed in the infrared by the extremum of $V(\chi)$ at $\chi = 0$, and all the masses and decay constants vanish in the limit $m = 0$. Additional lattice ensembles with small fermion mass and large β will be helpful to confirm this preliminary conclusion.

IV. SUMMARY AND DISCUSSION

We employed dilaton effective field theory (dEFT) as a diagnostic tool to discriminate between infrared-conformal and near-conformal, confining gauge theories. Our approach draws on spectroscopic lattice measurements performed with finite mass for the elementary fermions, in a range of parameter space in which both the pNGBs and the dilaton are clearly lighter than other states. This feature is expected to emerge naturally in theories near the lower edge of the conformal window, for small enough fermion masses. We took the dEFT to apply smoothly through the transition between confinement and conformality.

We tested this approach with two lattice studies meeting these requirements. For the $SU(3)$ gauge theory coupled to $N_f = 8$ Dirac fermions in the fundamental representation, we used measurements obtained with staggered fermions, restricted to the largest available lattice couplings and volumes [17, 18], to infer that the theory is outside the conformal window (near-conformal but confining in the $m \rightarrow 0$ limit). For the $SU(2)$ theory with $N_f = 1$ fermions in the adjoint representation, we used data obtained with Wilson fermions [7, 28], by restricting attention to ensembles in which the relevant masses are significantly smaller than the lattice cutoff, to minimize lattice artifacts. Our analysis indicates that this theory is inside the conformal window (infrared conformal in the $m \rightarrow 0$ limit).

We made several simplifying assumptions. We ignored systematic effects in the lattice measurements, such as correlations between individual measurements, and contamination from finite-volume and finite size effects. We included only leading-order terms in the dEFT Lagrangian. We verified explicitly that the lattice measurements employed small enough fermion masses to explore only small-field dEFT excursions.

Our results should be taken as preliminary, as indicated by the large uncertainty in some of the output—in particular the scaling dimension Δ . Future precision lattice measurements, particularly for the $SU(2)$ theory, could overcome these limitations, by exploring lattice parameters with smaller fermion masses and less contamination from lattice artifacts. Our framework can be applied to other gauge theories. It would be interesting, for example, to perform our analysis on lattice measurements

TABLE III. Numerical lattice measurements taken from Table IX of Ref. [17] with $\beta = 4.8$ (see also the data release [59]), for the $SU(3)$ theory coupled to $N_f = 8$ fermions transforming in the fundamental representation. The errors in parenthesis includes statistical and systematics, but correlations are neglected. The fermion mass, am , appears as a parameter in the lattice staggered action, and hence there is no associated uncertainty.

am	aM_π	aF_π	aM_d
0.00889	0.2253(37)	0.05262(88)	0.301(12)
0.0075	0.2057(34)	0.04831(80)	0.2744(85)
0.005	0.1657(27)	0.03982(66)	0.2408(87)
0.00222	0.1087(18)	0.02794(47)	0.1545(83)
0.00125	0.0811(13)	0.02168(36)	0.1174(48)

in the $SU(3)$ theory coupled to sextet fermions [20–25], or theories in other gauge groups, such as $Sp(4)$ [4, 6].

ACKNOWLEDGMENTS

We thank Ed Bennett and Biagio Lucini for useful discussions. The work of M.P. has been supported in part by the STFC Consolidated Grants No. ST/T000813/1 and ST/X000648/1. M.P. received funding from the European Research Council (ERC) under the European Union’s Horizon 2020 research and innovation program under Grant Agreement No. 813942. J.I. has been supported by STFC under grants No. ST/X000745/1 and No. ST/X003167/1.

Research Data Access Statement—The data generated for this manuscript can be downloaded from Ref. [64].

Open Access Statement—For the purpose of open access, the authors have applied a Creative Commons Attribution (CC BY) license to any Author Accepted Manuscript version arising.

Appendix A: Maximum likelihood analysis and lattice data

We here collect some technical details needed to reproduce our main results. First, we summarize in Tables III and IV the spectroscopic measurements for pNGBs and dilaton, taken from Refs. [17] and [28]. These measure-

ments are combined with Eqs. (9), (10), and (11), to define the χ^2 , in the following way.

Given the N fitting functions, $\vec{f} = \{f_i\}_{i=1}^N$, which depend on the K parameters of the model, $\vec{a} = \{a_k\}_{k=1}^K$,

TABLE IV. Numerical lattice measurements for the $SU(2)$ theory coupled to $N_f = 1$ fermion transforming in the adjoint representation [28, 60, 61], for ensembles with $\beta = 2.1$, and the largest available volumes. The errors in parenthesis are statistical only, and correlations are neglected. These numerical results are obtained with Wilson fermions, hence a measure of symmetry breaking effects due to finite fermion mass is provided by the PCAC mass, am_{PCAC} , extracted according to the process described in Ref. [62].

am_{PCAC}	aM_π	aF_π	aM_d
0.15326(21)	0.97363(51)	0.38982(94)	0.847(34)
0.13820(17)	0.92461(45)	0.37075(71)	0.716(57)
0.12200(23)	0.86745(64)	0.34875(92)	0.690(38)
0.10251(16)	0.79101(51)	0.31313(97)	0.565(36)
0.08011(19)	0.69504(63)	0.27437(70)	0.469(33)
0.04969(12)	0.53319(48)	0.20450(67)	0.373(29)
0.03246(14)	0.42018(32)	0.15925(36)	0.295(13)

and on M experimentally measurable quantities, $\vec{x} = \{x_j\}_{j=1}^M$, we define the $N \times N$ covariance matrix $\bar{\mathcal{C}}$ as

$$\bar{\mathcal{C}} \equiv O^T \mathcal{C} O, \quad (\text{A1})$$

where \mathcal{C} is the $M \times M$ covariance matrix of the observables, and $O_j^i = \frac{\partial f_i}{\partial x_j}$ is the $M \times N$ matrix of partial derivatives. The χ^2 function is the following

$$\chi^2(\vec{a}) \equiv \vec{f}^T(\vec{a}, \vec{x}) \bar{\mathcal{C}}^{-1} \vec{f}(\vec{a}, \vec{x}), \quad (\text{A2})$$

The best fit value for \vec{a} is obtained by minimizing numerically the function $\chi^2(\vec{a})$.

As we do not have access to the covariance matrix for the measurements listed in Tables III and IV, we take \mathcal{C} to be diagonal, with non-vanishing elements given by the variance due to the statistical errors of the measurements, σ_j^2 . We do not include systematic effects, assuming that they are smaller than the statistical ones, for those measurements we retain in the analysis. The functions f_i are defined by the left-hand side of Eqs. (9), (10), and (11), respectively. For the $SU(3)$ theory, we treat the 5 measurements of aM_π , aF_π , and aM_d as the observables. The five choices of am are treated as numerical values of a parameter that is known without uncertainty — the mass of the staggered fermions in the lattice action. For the $SU(2)$ theory, our χ^2 analysis makes use of the measurements of am_{PCAC} , aM_π , aF_π , and aM_d , restricting attention to the three ensembles with the lightest masses, among those with $\beta = 2.1$.

- [1] T. Banks and A. Zaks, *On the Phase Structure of Vector-Like Gauge Theories with Massless Fermions*, *Nucl. Phys. B* **196** (1982) 189.
- [2] K. Rummukainen and K. Tuominen, *Lattice Computations for Beyond Standard Model Physics*, *Universe* **8** (2022) 188.
- [3] H.S. Chung and D. Negradi, *f_0/m_0 and f_π/m_0 ratios and the conformal window*, *Phys. Rev. D* **107** (2023) 074039 [2302.06411].
- [4] E. Bennett et al., *Symplectic lattice gauge theories in the grid framework: Approaching the conformal window*, *Phys. Rev. D* **108** (2023) 094508 [2306.11649].
- [5] D. Negradi and H.S. Chung, *Mesonic decay constant and mass ratios and the conformal window*, *PoS LATTICE2023* (2024) 084 [2311.08668].
- [6] E. Bennett, D.K. Hong, H. Hsiao, J.-W. Lee, C.J.D. Lin, B. Lucini et al., *Meson spectroscopy in the $Sp(4)$ gauge theory with three antisymmetric fermions*, *Phys. Rev. D* **111** (2025) 074511 [2412.01170].
- [7] A. Athenodorou, E. Bennett, G. Bergner, P. Butti, J. Lenz and B. Lucini, *$SU(2)$ gauge theory with one and two adjoint fermions towards the continuum limit*, **2408.00171**.
- [8] T. Appelquist, G.T. Fleming and E.T. Neil, *Lattice study of the conformal window in QCD-like theories*, *Phys. Rev. Lett.* **100** (2008) 171607 [0712.0609].
- [9] A. Deuzeman, M.P. Lombardo and E. Pallante, *The Physics of eight flavours*, *Phys. Lett. B* **670** (2008) 41 [0804.2905].
- [10] Z. Fodor, K. Holland, J. Kuti, D. Negradi and C. Schroeder, *Nearly conformal gauge theories in finite volume*, *Phys. Lett. B* **681** (2009) 353 [0907.4562].
- [11] LATKMI collaboration, *Light flavor-singlet scalars and walking signals in $N_f = 8$ QCD on the lattice*, *Phys. Rev. D* **96** (2017) 014508 [1610.07011].
- [12] T. Appelquist et al., *Strongly interacting dynamics and the search for new physics at the LHC*, *Phys. Rev. D* **93** (2016) 114514 [1601.04027].
- [13] LATTICE STRONG DYNAMICS collaboration, *Nonperturbative investigations of $SU(3)$ gauge theory with eight dynamical flavors*, *Phys. Rev. D* **99** (2019) 014509 [1807.08411].
- [14] A.Y. Kotov, D. Negradi, K.K. Szabo and L. Szikszai, *More on the flavor dependence of m_ρ/f_π* , *JHEP* **07** (2021) 202 [2107.05996].
- [15] LATTICE STRONG DYNAMICS (LSD) collaboration, *Goldstone boson scattering with a light composite scalar*, *Phys. Rev. D* **105** (2022) 034505 [2106.13534].
- [16] A. Hasenfratz, *Emergent strongly coupled ultraviolet fixed point in four dimensions with eight Kähler-Dirac fermions*, *Phys. Rev. D* **106** (2022) 014513 [2204.04801].
- [17] LATTICE STRONG DYNAMICS collaboration, *Light scalar meson and decay constant in $SU(3)$ gauge theory with eight dynamical flavors*, *Phys. Rev. D* **110** (2024) 054501 [2306.06095].
- [18] LSD collaboration, *Hidden conformal symmetry from the lattice*, *Phys. Rev. D* **108** (2023) L091505 [2305.03665].
- [19] LATKMI collaboration, *Novel view of the flavor-singlet spectrum from multi-flavor QCD on the lattice*, *Phys. Rev. D* **112** (2025) 114503 [2505.08658].
- [20] Z. Fodor, K. Holland, J. Kuti, D. Negradi, C. Schroeder and C.H. Wong, *Can the nearly conformal sextet gauge model hide the Higgs impostor?*, *Phys. Lett. B* **718** (2012) 657 [1209.0391].
- [21] Z. Fodor, K. Holland, J. Kuti, S. Mondal, D. Negradi and C.H. Wong, *Toward the minimal realization of a light composite Higgs*, *PoS LATTICE2014* (2015) 244 [1502.00028].
- [22] Z. Fodor, K. Holland, J. Kuti, S. Mondal, D. Negradi and C.H. Wong, *Status of a minimal composite Higgs theory*, *PoS LATTICE2015* (2016) 219 [1605.08750].
- [23] Z. Fodor, K. Holland, J. Kuti, D. Negradi and C.H. Wong, *The twelve-flavor β -function and dilaton tests of the sextet scalar*, *EPJ Web Conf.* **175** (2018) 08015 [1712.08594].
- [24] Z. Fodor, K. Holland, J. Kuti and C.H. Wong, *Tantalizing dilaton tests from a near-conformal EFT*, *PoS LATTICE2018* (2019) 196 [1901.06324].
- [25] Z. Fodor, K. Holland, J. Kuti and C.H. Wong, *Dilaton EFT from p -regime to RMT in the ϵ -regime*, *PoS LATTICE2019* (2020) 246 [2002.05163].
- [26] A. Athenodorou, E. Bennett, G. Bergner and B. Lucini, *Infrared regime of $SU(2)$ with one adjoint Dirac flavor*, *Phys. Rev. D* **91** (2015) 114508 [1412.5994].
- [27] A. Athenodorou, E. Bennett, G. Bergner, D. Elander, C.J.D. Lin, B. Lucini et al., *Large mass hierarchies from strongly-coupled dynamics*, *JHEP* **06** (2016) 114 [1605.04258].
- [28] A. Athenodorou, E. Bennett, G. Bergner and B. Lucini, *Investigating the conformal behavior of $SU(2)$ with one adjoint Dirac flavor*, *Phys. Rev. D* **104** (2021) 074519 [2103.10485].
- [29] S. Matsuzaki and K. Yamawaki, *Dilaton Chiral Perturbation Theory: Determining the Mass and Decay Constant of the Technidilaton on the Lattice*, *Phys. Rev. Lett.* **113** (2014) 082002 [1311.3784].
- [30] M. Golterman and Y. Shamir, *Low-energy effective action for pions and a dilatonic meson*, *Phys. Rev. D* **94** (2016) 054502 [1603.04575].
- [31] A. Kasai, K.-i. Okumura and H. Suzuki, *A dilaton-pion mass relation*, **1609.02264**.
- [32] M. Hansen, K. Langåble and F. Sannino, *Extending Chiral Perturbation Theory with an Isosinglet Scalar*, *Phys. Rev. D* **95** (2017) 036005 [1610.02904].
- [33] M. Golterman and Y. Shamir, *Effective pion mass term and the trace anomaly*, *Phys. Rev. D* **95** (2017) 016003 [1611.04275].
- [34] T. Appelquist, J. Ingoldby and M. Piai, *Dilaton EFT Framework For Lattice Data*, *JHEP* **07** (2017) 035 [1702.04410].
- [35] T. Appelquist, J. Ingoldby and M. Piai, *Analysis of a Dilaton EFT for Lattice Data*, *JHEP* **03** (2018) 039 [1711.00067].
- [36] O. Catà, R.J. Crewther and L.C. Tunstall, *Crawling technicolor*, *Phys. Rev. D* **100** (2019) 095007 [1803.08513].
- [37] M. Golterman and Y. Shamir, *Large-mass regime of the dilaton-pion low-energy effective theory*, *Phys. Rev. D* **98** (2018) 056025 [1805.00198].
- [38] O. Catà and C. Müller, *Chiral effective theories with a*

- light scalar at one loop, *Nucl. Phys. B* **952** (2020) 114938 [1906.01879].
- [39] T. Appelquist, J. Ingoldby and M. Piai, *Dilaton potential and lattice data*, *Phys. Rev. D* **101** (2020) 075025 [1908.00895].
- [40] M. Golterman, E.T. Neil and Y. Shamir, *Application of dilaton chiral perturbation theory to $N_f = 8$, SU(3) spectral data*, *Phys. Rev. D* **102** (2020) 034515 [2003.00114].
- [41] M. Golterman and Y. Shamir, *Explorations beyond dilaton chiral perturbation theory in the eight-flavor SU(3) gauge theory*, *Phys. Rev. D* **102** (2020) 114507 [2009.13846].
- [42] T. Appelquist, J. Ingoldby and M. Piai, *Dilaton Effective Field Theory*, *Universe* **9** (2023) 10 [2209.14867].
- [43] A.A. Migdal and M.A. Shifman, *Dilaton Effective Lagrangian in Gluodynamics*, *Phys. Lett. B* **114** (1982) 445.
- [44] S. Coleman, *Aspects of Symmetry: Selected Erice Lectures*, Cambridge University Press, Cambridge, U.K. (1985), 10.1017/CBO9780511565045.
- [45] W.D. Goldberger, B. Grinstein and W. Skiba, *Distinguishing the Higgs boson from the dilaton at the Large Hadron Collider*, *Phys. Rev. Lett.* **100** (2008) 111802 [0708.1463].
- [46] T. Appelquist, J. Ingoldby and M. Piai, *Nearly Conformal Composite Higgs Model*, *Phys. Rev. Lett.* **126** (2021) 191804 [2012.09698].
- [47] T. Appelquist, J. Ingoldby and M. Piai, *Composite two-Higgs doublet model from dilaton effective field theory*, *Nucl. Phys. B* **983** (2022) 115930 [2205.03320].
- [48] G. Cacciapaglia, D.Y. Cheong, A. Deandrea, W. Isnard and S.C. Park, *Composite hybrid inflation: dilaton and waterfall pions*, *JCAP* **10** (2023) 063 [2307.01852].
- [49] T. Appelquist, J. Ingoldby and M. Piai, *Dilaton forbidden dark matter*, *Phys. Rev. D* **110** (2024) 035013 [2404.07601].
- [50] S. Bruggisser, B. von Harling, O. Matsedonskyi and G. Servant, *Dilaton at the LHC: complementary probe of composite Higgs*, *JHEP* **05** (2023) 080 [2212.00056].
- [51] R. Alonso, S. Chattopadhyay and J. Ingoldby, *The Potential of HEFT and the scale of New Physics*, 2512.13612.
- [52] J.E. Wu and Q.S. Yan, *Confront a dilaton model with the LHC measurements*, 2501.07820.
- [53] R. Zwicky, *QCD with an infrared fixed point and a dilaton*, *Phys. Rev. D* **110** (2024) 014048 [2312.13761].
- [54] A.F. Faedo, C. Hoyos, M. Piai, R. Rodgers and J.G. Subils, *Light holographic dilatons near critical points*, *Phys. Rev. D* **110** (2024) 126017 [2406.04974].
- [55] D. Elander, A.F. Faedo, M. Piai, R. Rodgers and J.G. Subils, *Light dilaton near critical points in top-down holography*, 2502.19226.
- [56] C. Cresswell-Hogg, D.F. Litim and R. Zwicky, *Dilaton Physics from Asymptotic Freedom*, 2502.00107.
- [57] R. Stegeman and R. Zwicky, *Gravitational D-Form Factor: The σ -Meson as a Dilaton confronted with Lattice Data*, 2508.18537.
- [58] R. Stegeman and R. Zwicky, *Gluon Gravitational D-Form Factor: The σ -Meson as a Dilaton confronted with Lattice Data II*, 2512.12315.
- [59] G.T. Fleming and et al. (Lattice Strong Dynamics (LSD)), *Dataset for "light scalar meson and decay constant in su(3) gauge theory with eight dynamical flavors"*, 2023. <https://dx.doi.org/10.5281/zenodo.8007955>.
- [60] A. Athenodorou, E. Bennett, G. Bergner and B. Lucini, *Investigating the conformal behaviour of su(2) with one adjoint dirac flavor — data release*, 2021. doi:10.5281/zenodo.5139618.
- [61] A. Athenodorou, E. Bennett, G. Bergner, J. Lenz and B. Lucini, *Su(2) gauge theory with one and two adjoint fermions towards the continuum limit — data release*, 2024. doi:10.5281/zenodo.13128505 (2024).
- [62] L. Del Debbio, B. Lucini, A. Patella and C. Pica, *Quenched mesonic spectrum at large N*, *JHEP* **03** (2008) 062 [0712.3036].
- [63] A.G. Cohen and H. Georgi, *Walking Beyond the Rainbow*, *Nucl. Phys. B* **314** (1989) 7.
- [64] T. Appelquist, J. Ingoldby and M. Piai, "Dilaton effective field theory across the conformal edge—data release."